The International Journal of Advanced Manufacturing Technology (2018) 99:1927–1936
https://doi.org/10.1007/s00170-018-2609-2

ORIGINAL ARTICLE

Taguchi approach for the optimization of refill friction stir spot welding parameters for AA2198-T8 aluminum alloy

Camila Caroline de Castro [1] · Athos Henrique Plaine [1] · Nelson Guedes de Alcântara [1] · Jorge Fernandez dos Santos [2]

Received: 6 May 2018 / Accepted: 15 August 2018 / Published online: 29 August 2018

Abstract

The present study features analytical and experimental results of AA2198-T8 joints produced by the refill friction stir spot welding of 1.6-mm-thick sheets. The selection of proper parameters for this process, such as tool rotational speed (RS), welding time (WT), and tool plunge depth (PD), played an important role in assuring weld strength. In this work, experimental tests were carried out based on the welding conditions according to Taguchi method, in order to determine optimal welding parameters and investigate the effect of those in the joint's mechanical properties and welded area. Results based on lap shear strength showed that RS and PD were responsible for more than 80% of strength variance, while the analysis based on the stir zone area measurement of the welds endorsed that WT had an insignificant contribution to the strength. Higher strength was correlated to bigger stir zone area, which results from higher RS and PD values.

Keywords Refill friction stir spot welding · Aerospace materials · Aluminum alloy · Taguchi method

1 Introduction

Refill friction stir spot welding (RFSSW), also known as friction spot welding (FSpW), is a relatively new solid state welding technique developed and patented by Helmholtz-Zentrum Geesthacht (former GKSS Forschungszentrum) to join similar or dissimilar lightweight materials, such as aluminum, magnesium, titanium, and thermoplastics [1], with the advantage of lacking residual keyhole in comparison with other friction spot-based techniques, such as friction stir spot welding (FSSW) [2, 3]. It presents itself as an excellent alternative for producing overlapped welds in aircraft and automotive industry because it provides lighter structures when compared with riveting, the most widely used technique to join materials in the transportation sector [2]. Besides, as RFSSW is solid state technique, defects associated with conventional fusion welding processes—such as resistance spot welding (RSW) and laser spot welding (LSW)—are avoided, what is

Highlights
- Refill friction stir spot welding of AA2198-T8 single-lap joints was demonstrated
- Welds produced by RFSSW in the experiment are suitable for aircraft application
- Stir zone area has a major influence on mechanical properties among geometric features
- Rotational speed and plunge depth variation influence the most lap shear strength outputs

✉ Camila Caroline de Castro
camila.ccastro@outlook.com

Athos Henrique Plaine
athosplaine@hotmail.com

Nelson Guedes de Alcântara
nelsong@ufscar.br

Jorge Fernandez dos Santos
jorge.dos.santos@hzg.de

[1] Department of Materials Engineering (DEMa), Federal University of Sao Carlos (UFSCar), Sao Carlos, Sao Paulo, Brazil

[2] Helmholtz Zentrum Geesthacht GmbH (HZG), Institute of Materials Research, Materials Mechanics, Solid State Joining Processes (WMP), Geesthacht, Schleswig, Holstein,, Germany

particularly interesting for aluminum high-strength alloys because of the presence of higher melting temperature oxides and hydroxides and their lower thermal conductivity in comparison with the base material [1].

The RFSSW process employs a three-piece non-consumable tool (clamping ring, sleeve, and pin, as shown in Fig. 1). For the sleeve plunge process variation (Fig. 2), two overlapped sheets are held together by the force of the clamping ring, while the rotational sleeve plunges into the material, what results in both heat generation due to the friction between tool and the base material and plastic deformation of the metal. The pin plays the role of accommodating the displaced material because of the sleeve plunge. During the sleeve plunge, the rotating pin is displaced towards the opposite plunge direction, creating a cavity to receive the displaced volume of material. After a selected welding time, both sleeve and pin are moved back to the sheet surface, what leads to an empty volume caused by sleeve retraction and its simultaneous refilling as a result of the pushing of the displaced material by the pin back into the sheet. In the final stage, the tool assembly is removed from the sheet's surface, resulting in a spot weld with no keyhole.

Fig. 1 RFSSW tool: pin, sleeve and clamping ring on the left, and tool assembly

Joints produced by the RFSSW process present different regions—the stir zone (SZ), the thermo-mechanically affected zone (TMAZ), and the heat-affected zone (HAZ) (Fig. 3)—characterized by particular microstructures in terms of size and grain orientation as a consequence of different deformation rates and temperature gradients. Stir zone is the region where very fine recrystallized grains are found because of the combination between high shear rates and process temperature that results from tool stirring contact and it corresponds to the center region of the weld [1]. Heat-affected zone is the region adjacent to the base material, which does not experience plastic deformation while it is moderately affected by the heat input, leading to the recovery of rolled microstructure [4]. Finally, thermo-mechanically affected zone is the region between SZ and HAZ that experiences moderate plastic deformation and heat input, which are not in sufficient levels to induce the recrystallization phenomenon on the region, resulting in an elongated-and-deformed-grained microstructure [4–7].

Lightweight aluminum alloys are widely used in the automotive and aerospace industries for the reduction of structure weight and fuel consumption as a result of specific properties, such as resistance and low density [8, 9]. Because lithium is a metal with very low density (0.534 g/cm^3), its addition to aluminum enables the reduction of Al alloys' density: additions of 1% in weight of Li provide a decrease of 3% in density. Besides, Li additions to aluminum alloys modify their mechanical properties, such as Young's modulus (e.g., 1% wt. Li addition provides 6% increase in Young's modulus), hardness (formation of hardening precipitates), and fatigue crack resistance (higher fatigue crack growth resistance) [9]. In this context, aiming aircraft and space applications, the AA2198—an Al-Cu-Li alloy—was developed by Reynolds Metal Company and McCook Metals in 2005 [9].

Design of experiment (DOE) techniques have many potential uses in improving processes and products. However, some classical DOE techniques may be too complex and difficult to use because of their requirements related to a large number of experiments, which considerably increases with the number of aimed parameters to be investigated [10]. To minimize this complexity, several authors have reported works on the optimization of RFSSW process parameters using Taguchi method to design experiments. The Taguchi approach is a simple and powerful statistical technique for optimizing solid state welding processes because its particular orthogonal array design enables the analysis of the entire parameter space using a reduced number of experiments [3, 10]. When used along with analysis of variance (ANOVA), Taguchi can be helpful to determine the relative influence of each welding parameter on weld properties, and to obtain the optimal process combination of parameters for the aimed response [2].

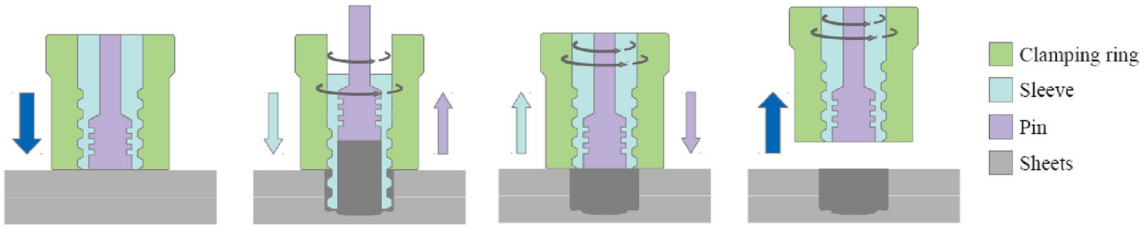

Fig. 2 Schematic illustration of the four stages of RFSSW sleeve plunge variant. **a** Clamping of the sheets. **b** Sleeve plunging and pin retraction. **c** Pin and sleeve placed back to the sheet surface. **d** Tool assembly removal

The feasibility of RFSSW and influence of welding parameters variation on the mechanical performance of lightweight materials joints has been widely documented on the literature. Pieta et al. [5] studied the welding parameters optimization for the joint of AA2198-T8 3.2-mm-thick sheets and found out that intermediate levels of rotational speed associated with highest levels of welding time and plunge depth (2000 rpm, 10 s, and 4.7 mm) produce welds with the highest lap shear strength among the analyzed parameters. Similar conclusion was obtained by Shi et al. [11] in a study of RFSSW on 2-mm-thick sheets of the same material, which also indicates that the most resistant welds were achieved by intermediate levels of rotational speed (1800 rpm), among the selected range of parameters. For the welding of AA2198 thinner sheets, however, the influence of welding parameters variation on joints' mechanical performance is yet to be investigated.

Amancio et al. [1] suggested that larger welds produce stronger joints. However, to the best of our knowledge, there are no published studies addressing the investigation of this relation between the stir zone area of a cross section and the mechanical performance of a weld, as well as what mechanisms are affected by this feature such as failure mode.

This work aims to study the optimized welding condition of AA2198-T8 1.6-mm sheets overlapped joints produced by refill friction stir spot welding based on the Taguchi approach, by systematically investigating the influence of important process parameters (rotational speed, welding time, and plunge depth) on the lap shear strength of the produced joints, correlating, for the first time, the resistance of each weld with its stir zone area.

2 Materials and methods

2.1 Lap shear strength test

The material used for this study is a 1.6-mm sheet of Al-Cu-Li 2198 alloy—3.4%wt Cu, 1.01%wt Li, 0.33%wt Mg, 0.22%wt Ag, and 0.11%wt Zr balanced with Al—heat treated under T8 condition (solution heat treatment, cold work, then artificial aging) [12]. The specimens for the lap shear strength test were produced by welding two 126 mm (length) × 35 mm (width) × 1.6 mm (thickness) sheets in a lap configuration, according to the ISO 14273 standard, with an overlap of 46 mm [13]. For the refill friction stir spot weld process, joints were produced by a RPS 100 FSpW machine using the sleeve plunge process variant, with a clamping force of 14.6 kN. Lap shear tests were performed with a screw-drive Zwick-Roell 1478 testing machine, with a load capacity of 200 kN and constant displacement rate of 1 mm/min.

2.2 Statistical analysis—DOE and ANOVA

Preliminary experiments were performed to reach feasible maximum and minimum levels for the three factors of RFSSW—tool rotational speed (RS), welding time (WT), and tool plunge depth (PD)—to be used in the Taguchi analysis. The criteria for the definition of parameters were based on the absence of severe volumetric defects on the welds, followed by the lap joints' mechanical resistance of and review of previous works on friction-based processes [5, 14]. The one-factor-at-a-time (OFAT) technique—only one factor at a time is varied, while others are kept fixed—was used; rotational speed and welding time were tested in four different levels each, and plunge depth was tested in three different conditions.

Taguchi approach was applied in order to optimize the effects of welding parameters. These parameters are called control factors because they are among the variables that can be specified during the friction spot welding process. Table 1 summarizes the factors and their levels used in this work. DOE based on orthogonal array was chosen once it is the smallest fractional factorial plan which still allows identifying the main effects of each factor with high efficiency, although

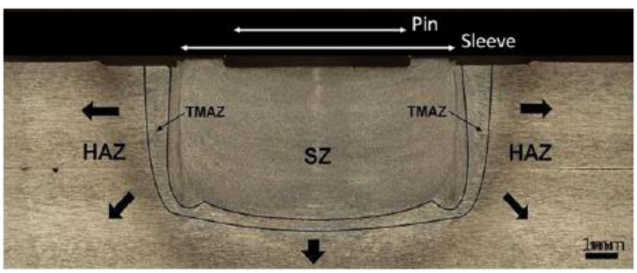

Fig. 3 Representative macrograph of a friction spot weld with three different regions: stir zone (SZ), thermo-mechanically affected zone (TMAZ), and heat-affected zone (HAZ) [5]

Table 1 RFSSW parameters and their levels

Factor	Level 1	Level 2	Level 3
Tool rotational speed (rpm)	1100	1300	1500
Welding time (s)	3	4	5
Tool plunge depth (mm)	2.1	2.6	2.8

the interaction between the factors is not taken into account [15]. The experiment was designed using a L9 orthogonal array, resulting in nine experiments—three factors with three levels each. All the nine experiments were run in triplicates. Lap shear strength (LSS) was taken as the performance metric for the Taguchi analysis, and the statistical study was generated using MINITAB® 18.

Taguchi method uses signal-to-noise ratio (SNR), a ratio between the desired response and its variance. The analysis of SNR enables highlighting the conditions in which the signal is significantly greater in comparison with the noise [15]. For the spot weld, it is desired the maximum response (LSS), and SNR was calculated based on the-larger-the-better category. The signal-to-noise ratio (η) is defined in as shown in Eq. 1 [10].

$$\eta = -10\log\left(\frac{1}{n}\sum_{i=1}^{n}\frac{1}{T_i 2}\right) \quad (1)$$

2.3 Macrographic examination

Macrographic analysis was performed in order to relate visual characteristics of the joints to the mechanical behavior for each condition given by the Taguchi method. Joints were cut 1 mm close to the weld symmetry plane, and the samples were manually grounded (grids 320, 600, 1200, 2500, and 4000) until it was guaranteed that the refereed plane was reached. For this purpose, samples were marked on their center and embedded in a soft transparent epoxy resin for clear visualization of the mark. Polished samples were etched by Keller's reagent (2 mL hydrofluoric acid 48%, 3 mL concentrated hydrochloric acid, 5 mL concentrated nitric acid, 190 mL distilled water). Macrographs were taken using a Leica DFC 295 camera attached to a DM IRM optical microscope. All area measurement was done using the ImageJ 1.51 k image analysis software: macrographs were treated in order to enhance the contrast between the stir zone and the other regions of the weld, based on the difference of shape and size of the grains. Binary images were build generating images with only black or white pixels for the easy isolation of the stir zone region (represented with black pixels), and subsequent counting of these pixels for the measurement of SZ.

Table 2 Experimental conditions for the Taguchi analysis (rotational speed, welding time, and plunge depth), mean of experimental results for lap shear strength test, and calculated signal-to-noise ratio for each welding condition

Welding condition	RS (rpm)	WT (s)	PD (mm)	Average LSS (N)	Signal-to-noise ratio
C1	1100	3	2.1	4877 ± 78	73.76
C2	1100	4	2.6	5733 ± 270	75.17
C3	1100	5	2.8	7685 ± 420	77.71
C4	1300	3	2.6	5799 ± 110	75.27
C5	1300	4	2.8	6996 ± 747	76.90
C6	1300	5	2.1	5650 ± 505	75.04
C7	1500	3	2.8	7947 ± 349	78.00
C8	1500	4	2.1	7426 ± 724	77.42
C9	1500	5	2.6	7498 ± 237	77.50

Data availability The raw and processed data required to reproduce these findings are available to download from https://doi.org/10.17632/ybnf33gfrs.1.

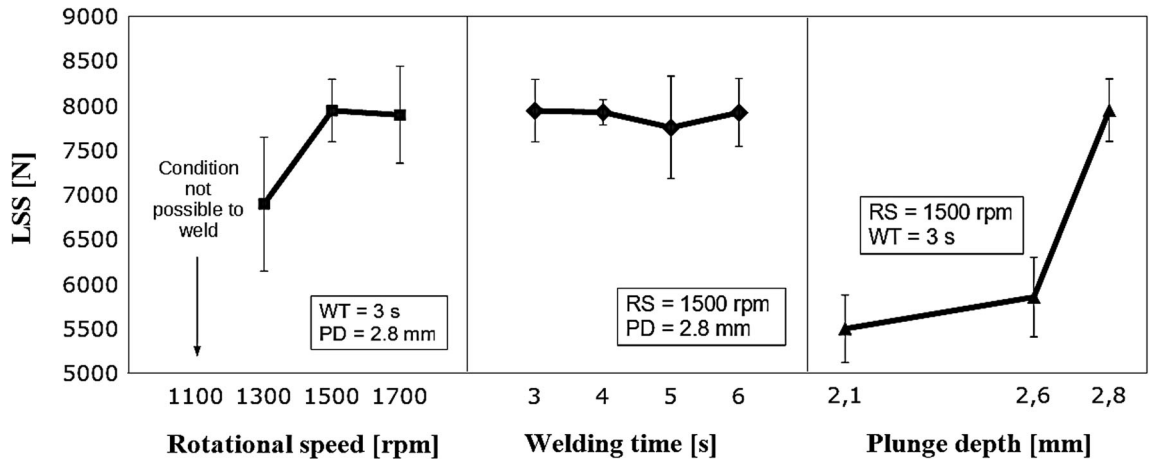

Fig. 4 Selection of upper and lower limit parameters to be applied on Taguchi method: plots of lap shear strength values versus levels for RS, WT, and PD

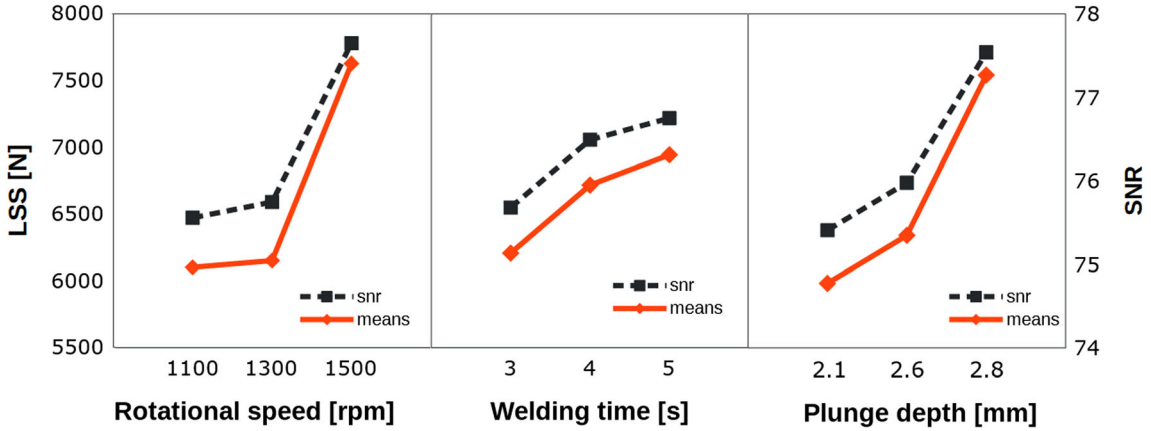

Fig. 5 Main effects plot of mean and signal-to-noise ratio for rotational speed, welding time, and plunge depth, based on LSS response

3 Results and discussion

3.1 Definition of parameter limits

Figure 4 shows plots of levels versus their LSS, for each one of the factors. Although the combination of RS = 1100 rpm/WT = 3 s/PD = 2.8 mm was not weldable due to the low heat input associated with high tool penetration rate, the RS lower limit could be defined as 1100 rpm since it provides enough heat input for plasticizing the material for smaller penetration rates (greater welding times and smaller plunge depth). For the upper limit, 1500 rpm was set since it is the highest rotational speed value after which LSS starts to decrease with the increase in RS. Campanelli et al. [3] associate this turning point in terms of RS to a decrease in the heat input, which is a function of torque. When the RS gets too high, material viscosity decreases, leading to a decrease in torque. Furthermore, according to Sabari et al., when the highest strength of the joint is aimed, this RS limitation may be related to the increase in grain size of stir zone because it increases with RS, as a result of the higher heat input in the material, which enables the growth of recrystallized grains [14]. Welding time does not present a great variation of LSS along the defined levels, as observed in the charts. Therefore, aiming industrial applications where reduced welding time leads to higher production rates; levels 3, 4, and 5 s were selected for this study. Finally, the limits of PD were selected from 2.1 to 2.8 mm because of the specimen configuration associated with sheet thickness, since each sheet is 1.6 mm thick, resulting in joints with 3.2 mm (two overlapped sheets).

Table 3 Optimized condition predicted by Taguchi method (C10) and its average lap shear strength value

Welding condition	RS (rpm)	WT (s)	PD (mm)	Average LSS (N)
C10	1500	5	2.8	7759 ± 428

3.2 Taguchi approach

Table 2 lists the results from the Taguchi L9 orthogonal array analysis, presenting LSS values along with calculated average mean and signal-to noise for each combination of RS, WT, and PD. The welds exhibited LSS values within 4877 ± 78 N (condition 1) and 7947 ± 349 N (condition 7). All the results from the LSS test exceeded the minimum value required for aeronautic application according to AWS D17.2 [16] (3180 N per weld), considering the ultimate tensile strength for AA22198-T8 160 MPa [9]. When aiming to achieve the best weld performance and quality, higher values for both mean values and SNR are desired because they lead to higher strength and less variability in the strength response. Table 2 states that the best combination of parameters is achieved by using the C7 condition (LSS = 7947 N and SNR = 78.00), which corresponds to the highest tool rotational speed and plunge depth levels used in the experiment (1500 rpm and 2.8 mm, respectively), but the lowest welding time (WT = 3 s).

The optimum welding condition predicted by Taguchi method is shown in Fig. 5. Three charts for LSS and SNR are presented, one for each factor—RS, WT, and PD—along with

Table 4 Analysis of variance and individual influence of rotational speed, welding time, and plunge depth in LSS in terms of means and SNR

	Factor	*df*	SS	MS	*F* value	%I
Mean	RS	2	4,505,750	2,252,875	8.33	46%
	WT	2	854,534	427,267	1.58	9%
	PD	2	540,734	1,997,842	7.39	40%
	Error	2	9,896,702	270,367	–	5%
SNR	RS	2	8.036	4.018	7.41	44%
	WT	2	1.882	0.941	1.73	10%
	PD	2	7.304	3.652	6.73	40%
	Error	2	1.085	0.542	–	6%

df degrees of freedom, *SS* sum of squares, *MS* mean square, *%I* percentage of influence

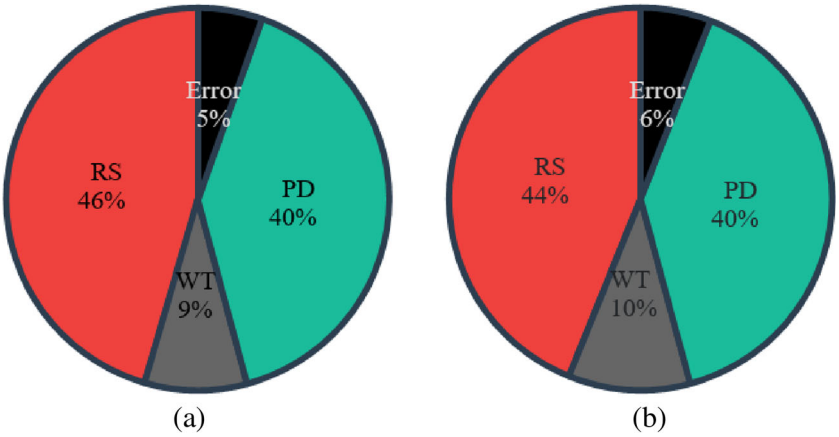

Fig. 6 Influence of individual parameters on the variance of LSS in terms of **a** means and **b** SNR

their levels. The highest point of each chart indicates the best level for the factor, based on LSS means and signal-to-noise ratio, what leads to the optimized condition for higher LSS values: 1500 rpm, 5 s, and 2.8 mm. In this manner, a new condition, C10, was welded and tested (Table 3) since this combination of parameters was not present on the Taguchi L9 orthogonal array previously designed. The statistical prediction was not very accurate in providing the ultimate combination of parameters for the highest strength of the joint because the C10 condition (1500 rpm, 5 s, 2.8 mm) presented a slightly lower LSS average when compared to C7 (1500 rpm, 3 s, 2.8 mm), which showed the best mechanical performance (Table 2). C7 and C10 consist of two combinations of parameters with identical RS and PD levels but different WT. As previously shown, WT itself has no significant influence on the LSS values for the used welding parameters range, which might explain the difference between the optimum parameters predicted by the Taguchi method and the results provided by lap shear strength test.

Considering that the Taguchi method provides the response of LSS mean and SNR for each factor and each level individually, the analysis of Fig. 5 allows understanding the influence of parameters on the joints' resistance. Taguchi outputs indicate the variation (delta-δ) between maximum and minimum SNR, and mean LSS value between the three levels for RS, WT, and PD. A comparison of delta values indicates the effectiveness of RS, PD, or WT in LSS: the higher the difference is, the more effective the factor on weld strength is. Similar mean and SNR delta were achieved for tool plunge depth and rotational speed (1558 versus 1525 N, in terms of means; 2.13 versus 2.09, in terms of SNR). The WT delta is significantly lower than the other two variables, which leads to a very small influence on LSS and SNR. Furthermore, each curve behavior presents discrepancies, although the response always increases along the levels. RS and PD presented similar trends: the second slope of the curve becomes steeper than the first one, unlike the WT behavior, which shows a slope angle

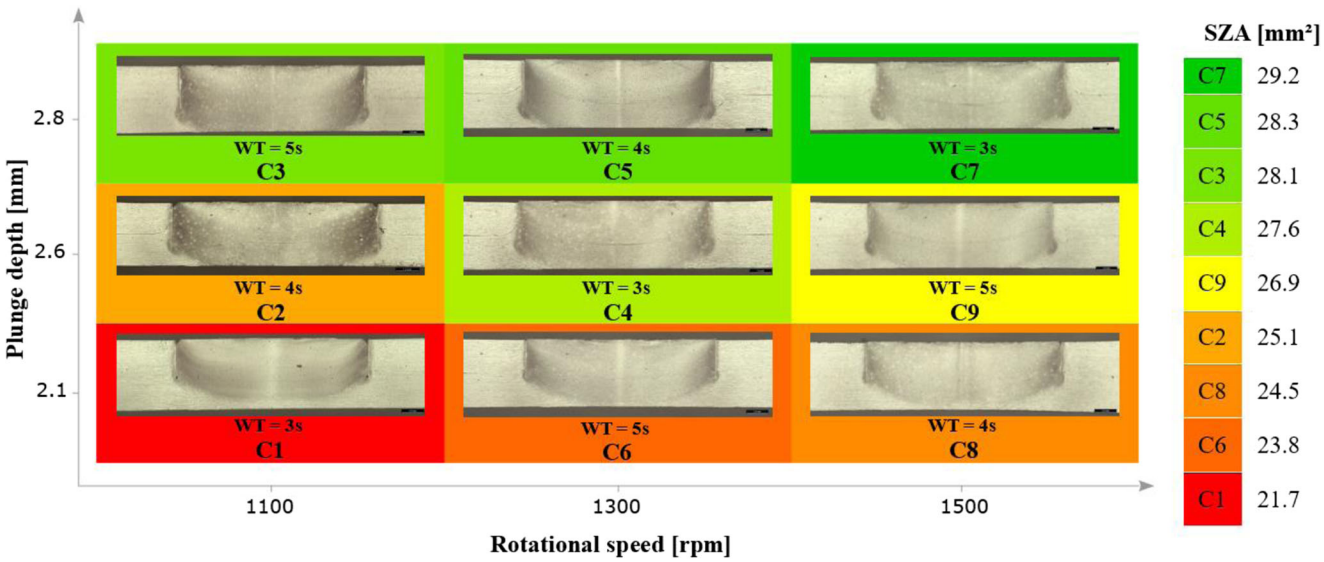

Fig. 7 RFSSW macrographs for different welding conditions. Color rating indicates weld area sizes, from lower values (red) to higher values (green) in mm^2

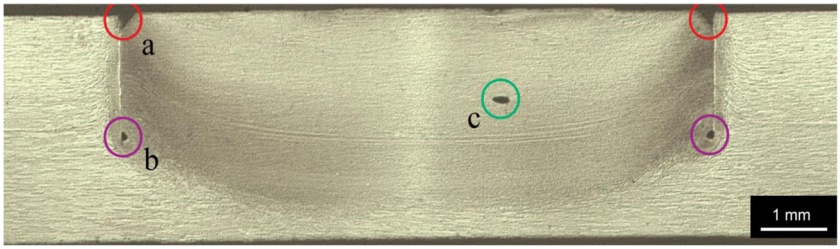

Fig. 8 Representative macrograph of a weld in which defects such as **a** incomplete refill, **b** lack of mixing, and **c** void can be observed

decrease between the two highest levels. In the portion between levels 2 and 3 for RS and PD, variations in the parameters lead to a higher response than the one expected for the same variation between levels 1 and 2. The opposite is expected for WT.

ANOVA (Table 4 and Fig. 6) of the influence of individual parameters on the lap shear strength performance indicates that RS and PD are the ultimate influencing factors on LSS (corresponding to 86% of contribution percentage (%I) altogether). Note that it is not accurate to affirm that RS has the greatest effectiveness on LSS because the contribution percentage values (%I) of RS and PD (46% for RS and 40% for PD, in terms of means) present an overlap as the process error value must be considered. These results suggest that both RS and PD are the most important factors for controlling LSS, especially when error is considered. Studies performed by Plaine et al. on dissimilar RFSSW of AA6168-T8 and Ti-6Al-4V [2] sheets and similar AA7975 friction spot welds of 0.8-mm-thick sheets reported by Kubit et al. [17] conclude that RS is responsible for the highest percentage of contribution on LSS variance, although results reported by Campanelli et al. [3] indicate that variations on PD levels provide the highest influence on the variance in weld resistance of AZ31 sheets. Furthermore, ANOVA indicates that WT variations result on an irrelevant contribution to LSS variation, both terms of means (9%) and SNR (10%), especially when compared with the error (5 and 6%, respectively). Other friction spot welds of similar light material joints also indicate WT as an irrelevant influence on LSS: Campanelli et al. [3] also report in the study of AZ31B-H24 Mg alloy 2-mm sheets that the WT percentage of contribution is significantly smaller than the error (4.38 versus 16.58%—for WT influence and ANOVA error, respectively, in terms of means; 6.55 versus 17.87%, in terms of SNR), which allows concluding that welding time shows no statistical influence on the strength of these joints for the welding parameter range used for this evaluation.

3.3 Macrographic analysis

As reported by Amancio et al., the mechanical performance of a friction spot joint is a function of metallurgical transformations, such as stir zone measured in terms of area [1], and other geometric characteristics, such as defects (voids, incomplete refill, among others) and hook angle [4].

Figure 7 shows cross sections of friction spot welded lap joints upon Taguchi L9 array conditions. The presence of defects, such as voids (C1), incomplete refill (C1, C2, and C3), and lack of mixing (C1), is observed only in samples with RS = 1100 rpm. These defects can be observed in a representative macrograph presented in Fig. 8. Since RS is of great importance on temperature and material flow for the joint, low tool rotational speed may not be able to produce defect-free and sound welds. That was the case for the welds produced with RS = 1100 rpm, which was not able to provide sufficient heat to plasticize the material. Kubit et al. also associate the formation of similar defects found in 0.8-mm aluminum sheet friction spot welding samples with inappropriate

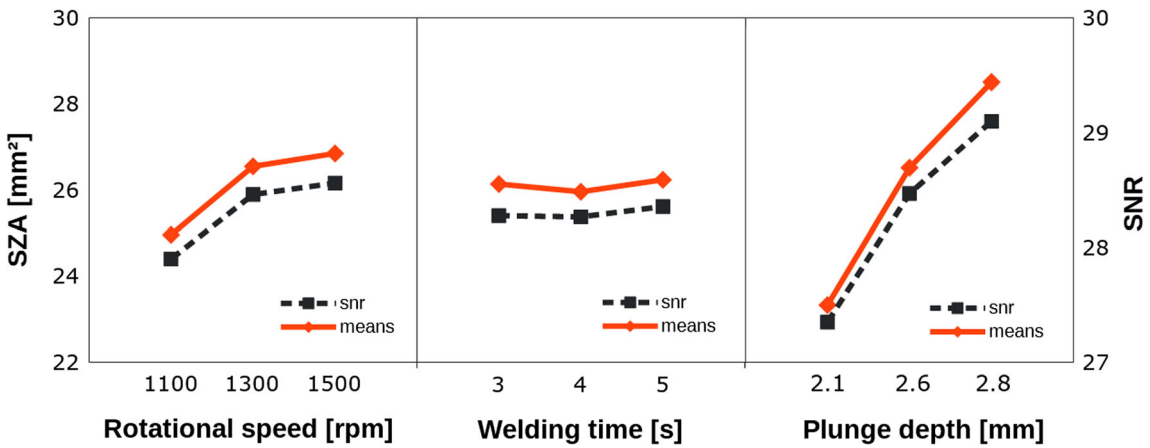

Fig. 9 Main effects plot of mean and signal-to-noise ratio for rotational speed, welding time, and plunge depth, based on SZA response

Table 5 Analysis of variance and individual influence of rotational speed, welding time, and plunge depth in SZA in terms of means and SNR

	Factor	*df*	SS	MS	*F* value	%I
Mean	RS	2	6.17	3.08	3.19	12.5%
	WT	2	0.12	0.06	0.06	0.2%
	PD	2	40.96	20.48	21.17	83.3%
	Error	2	1.94	1.94	–	3.9%
SNR	RS	2	0.76	0.38	2.91	13.2%
	WT	2	0.01	0.01	0.05	0.2%
	PD	2	4.72	2.36	18.15	82.1%
	Error	2	0.26	0.13	–	4.5%

df degrees of freedom, *SS* sum of squares, *MS* mean square, *%I* percentage of influence

process parameters, leading to material's poor flowability [17].

In Fig. 7, it is possible to see the variance in stir zone area (SZA) along the parameter variation, which is set in color scale from red (corresponding to the smallest area, 21.7 mm^2, for C1 condition) to green (for the largest area, 29.2 mm^2, for C7 condition). Minimum and maximum SZA values correspond to the minimum and maximum values of LSS (Table 2). In all cases, the stir zone area increases with plunge depth because of its direct influence on the height dimension of the welded area. The same occurs for the rotational speed evolution: higher values of RS lead to greater heat input and, consequently, to the plasticization of a larger volume of base material, which may experience the dynamic recrystallization phenomenon because of the combination of high plastic deformation and heat resulting in the stir zone. Welding time appears to have no significant influence on the weld area, except for the C4 and C9 samples, in which the rotational-speed-increasing-in-area effect was overlapped by another effect, most probably related to the longer welding time. Despite the presence of defects in welds produced with RS = 1100 rpm, the increase in area in the studied conditions evolves similarly with the LSS; i.e., the increase in LSS is not significantly affected by the presence of defects on the welds produced in this work. It suggests that stir zone area presents a more significant contribution to LSS than the presence of defects on the welds analyzed herein.

A comparison of delta values provided by the Taguchi analysis (Fig. 9) along with the ANOVA's percentage of contribution (Table 5 and Fig. 10) for means and signal-to-noise ratio indicates the factor effectiveness in SZA and, consequently, in weld strength because the stir zone area offers a major contribution to the resistance, as indicated by the LSS value. As seen in Figs. 9 and 10, considerable higher delta values and percentage of contribution for both means and SNR are found for tool plunge depth. A slight variation in tool plunge depth causes the greatest variation in SZA among the factors observed in this experiment, which is coherent with the observation of Fig. 5, since LSS is correlated to SZA. Hence, similar behavior of RS, WT, and PD is expected. RS is also significant for the SZA variance, as observed in the charts presented in Fig. 9—which were expected, according to the Taguchi analysis for weld strength. Finally, a variation in the levels of welding time does not implicate any influence on SZA values: Taguchi plots, as shown in Fig. 9, show almost no variation in means and SNR between its three levels, while ANOVA indicates the WT percentage of influence on SZA as 0.2%, which is even smaller than the error (3.5 and 4.5%). This can be explained by the thermal conduction through the thickness dimension of the sheet (vertical direction): as the selected material is a thin 1.6-mm sheet and aluminum has one of the highest thermal conductivity among metals, heat is very rapidly distributed through the volume of material adjacent to the plunge. A comparison with the analysis of variance presented by Pieta et al. [5] when AA2198-T8 3.2-mm-thick sheets joined by RFSSW were studied helps verifying the phenomenon: WT percentage of influence on welds' LSS increases along the thickness of the material, going from 0.2% for 1.6-mm sheets to 33% for 3.2-mm sheets. Since one

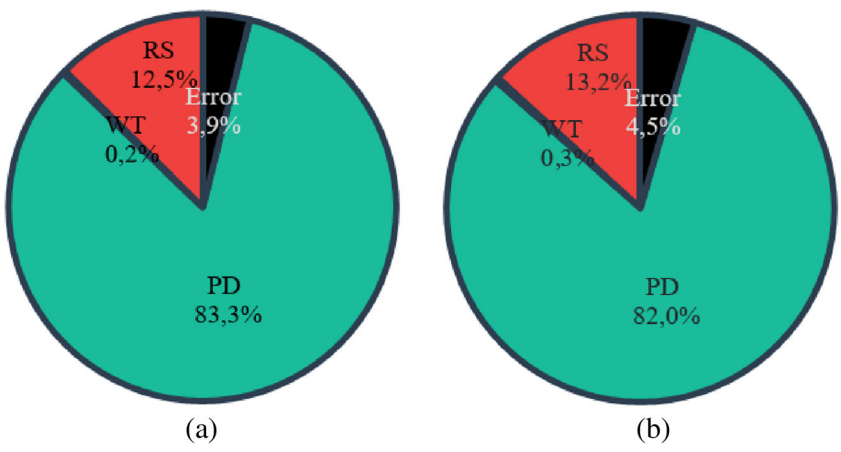

Fig. 10 Influence of individual parameters on the variance of SZA in terms of **a** means and **b** SNR

of these sheets is thicker, the time for a thermal equilibrium is greater, and the process is substantially more affected by WT. Therefore, thermal equilibrium is reached in a very short time for 1.6-mm thick, and the material's capability of plasticization is not affected by WT limitations considering the levels used in this work.

The Taguchi analysis for SZA (Fig. 9) predicts that the biggest SZA is achieved under RS = 1500 rpm, WT = 5 s, and PD = 2.8 mm, which is in accordance with the optimized condition predicted by the Taguchi analysis when highest values for LSS are aimed (C10 condition). However, since WT does not influence the SZA, the C7 is taken for the optimized condition, because it presents same RS and PD levels, with a smaller WT. That implicates on a reduction of 2 s on the welding process associated with the statistical guarantee of the optimum value of SZA and, consequently, with the best quality of weld in terms of strength.

4 Conclusions

The effects of the refill friction stir spot welding process parameters on the mechanical strength of AA2198-T8 aluminum alloy sheets were investigated using statistical and macrographic analysis. The following conclusions can be drawn based on the experimental and analytical results.

- All the welds produced with the combination of parameters based on Taguchi L9 orthogonal array demonstrated to be suitable for aeronautical application, presenting values for LSS which range from 4877 to 7947 N and exceeding the minimum required lap shear strength according to AWS D17.2 (3180 N).
- For the selected range of welding parameters, RS and PD were the parameters with the highest percentage of contribution on the lap shear strength of the joints, with 46 and 40%, respectively. In contrast, WT was shown to have no significant influence on the joints performance because its percentage of contribution was of no statistical significance.
- Macrostructural analysis has demonstrated to be a successful technique for relating geometric factors to LSS. Among the geometrical features analyzed, the stir zone area was observed to have a major and direct influence on the LSS of the welds, while the presence of volumetric defects on the joints, such as incomplete refill, voids, and lack of mixing, seems to have a lower influence on the produced joints.
- The parameter optimization, considering efficiency and economic matters, was shown to be C7 condition (RS = 1500 rpm, WT = 3 s, PD = 2.8 mm). Although Taguchi analysis has indicated a different condition (RS = 1500 rpm, WT = 5 s, PD = 2.8 mm), LSS test results and SZA measurements endorses C7 as the optimized set of parameters. It should be noted that C7 and C10 (with very similar LSS values) consist in two combinations of parameters with identical levels for RS and PD. While they present different levels for WT, this parameter was previously shown to be of no significant influence on joint's mechanical performance.

Funding The authors would like to acknowledge the financial support provided by Helmholtz Association (Germany) and CNPq (National Council for Scientific and Technological Development, Brazil, process no. 134520/2017-3).

References

1. Amancio-Filho ST, Camillo AP, Bergmann L et al (2011) Preliminary investigation of the microstructure and mechanical behaviour of 2024 aluminium alloy friction spot welds. Mater Trans 52:985–991. https://doi.org/10.2320/matertrans L-MZ201126
2. Plaine AH, Gonzalez AR, Suhuddin UFH, dos Santos JF, Alcântara NG (2015) The optimization of friction spot welding process parameters in AA6181-T4 and Ti6Al4V dissimilar joints. Mater Des 83:36–41. https://doi.org/10.1016/j.matdes.2015.05.082
3. Campanelli LC, Suhuddin UFH, dos Santos JF, de Alcântara NG (2012) Parameters optimization for friction spot welding of AZ31 magnesium alloy by Taguchi method. Soldagem & Inspeção 17:26–31. https://doi.org/10.1590/S0104-92242012000100005
4. Rosendo T, Parra B, Tier MAD, da Silva AAM, dos Santos JF, Strohaecker TR, Alcântara NG (2011) Mechanical and microstructural investigation of friction spot welded AA6181-T4 aluminium alloy. Mater Des 32:1094–1100. https://doi.org/10.1016/j.matdes.2010.11.017
5. Pieta G, dos Santos J, Strohaecker TR, Clarke T (2014) Optimization of friction spot welding process parameters for AA2198-T8 sheets. Mater Manuf Process 29:934–940. https://doi.org/10.1080/10426914.2013.811727
6. Shen J, Lage SBM, Suhuddin UFH, Bolfarini C, dos Santos JF (2018) Texture development and material flow behavior during refill friction stir spot welding of AlMgSc. Metall Mater Trans A 49:241–254. https://doi.org/10.1007/s11661-017-4381-6
7. Reimann M, Goebel J, dos Santos JF (2017) Microstructure and mechanical properties of keyhole repair welds in AA 7075-T651 using refill friction stir spot welding. Mater Des 132:283–294. https://doi.org/10.1016/j.matdes.2017.07.013
8. Yang C-W, Hung F-Y, Lui T-S, Chen LH, Juo JY (2009) Weibull statistics for evaluating failure behaviors and joining reliability of friction stir spot welded 5052 aluminum alloy. Materials Tansactions 50:145–151. https://doi.org/10.2320/matertrans MRA2008341
9. Rioja RJ, Liu J (2012) The evolution of Al-Li Base products for aerospace and space applications. Metall Mater Trans A 43:3325–3337. https://doi.org/10.1007/s11661-012-1155-z
10. Bilici MK (2012) Application of Taguchi approach to optimize friction stir spot welding parameters of polypropylene. Mater Des 35:113–119. https://doi.org/10.1016/j.matdes.2011.08.033

11. Shi Y, Yue Y, Zhang L, Ji S, Wang Y (2018) Refill friction stir spot welding of 2198-T8 aluminum alloy. Trans Indian Inst Metals 71: 139–145. https://doi.org/10.1007/s12666-017-1146-2
12. Han J, Zhu Z, Li H, Gao C (2016) Microstructural evolution, mechanical property and thermal stability of Al–li 2198-T8 alloy processed by high pressure torsion. Mater Sci Eng A 651:435–441. https://doi.org/10.1016/j.msea.2015.10.112
13. International Organization for Standardization (2016) ISO 14273: 2016 - Resistance welding - Destructive testing of welds - Specimen dimensions and procedure for tensile shear testing resistance spot and embossed projection welds
14. Sree Sabari S, Malarvizhi S, Balasubramanian V (2016) Characteristics of FSW and UWFSW joints of AA2519-T87 aluminium alloy: effect of tool rotation speed. J Manuf Process 22:278–289. https://doi.org/10.1016/j.jmapro.2016.03.014
15. Ulrich KT, Eppinger SD (2015) Product design and development, 5th edn. McGraw-Hill Education, New York City
16. American Welding Society (2013) AWS D17.2/D17.2M:2013 - Specification for Resistance Welding for Aerospace Applications
17. Kubit A, Kluz R, Trzepieciński T, Wydrzyński D, Bochnowski W (2018) Analysis of the mechanical properties and of micrographs of refill friction stir spot welded 7075-T6 aluminium sheets. Archives of Civil and Mechanical Engineering 18:235–244. https://doi.org/10.1016/j.acme.2017.07.005